TABLE V. X-ray scattering factors. The HFS or HFS′ value closest to the HF value is starred. $s=\sin\theta/\lambda$ is in units of Å^{-1}.

s	HF[a]	HFS[b]	HFS′	H
0.00	18.00	18.00	18.00	18.00
0.05	17.54	17.57*	17.49	17.45
0.10	16.30	16.41*	16.16	16.03
0.15	14.65	14.84	14.47*	14.24
0.20	12.93	13.20	12.80*	12.51
0.25	11.42	11.70	11.35*	11.06
0.30	10.20	10.45	10.18*	9.93
0.35	9.25	9.46	9.27*	9.07
0.40	8.54	8.70	8.57*	8.43
0.50	7.56	7.64	7.57*	7.52
0.60	6.86	6.91	6.84*	6.83
0.70	6.23	6.30	6.22*	6.19
0.80	5.61	5.70	5.60*	5.55
0.90	5.01	5.11	5.00*	4.93
1.00	4.43	4.54	4.42*	4.34
1.10	3.90	4.01	3.89*	3.82
1.20	3.43	3.54	3.43*	3.35
1.30	3.03	3.13	3.03*	2.96

[a] *International Tables for X-ray Crystallography* (Kynoch Press, Birmingham, England, 1962), Vol. 3, p. 204.
[b] H. P. Hanson *et al.*, Acta Cryst. **17**, 1040 (1964). These scattering factors and our HFS′ scattering factors were computed from orbitals whose one-electron equations used a potential that was modified at large radii. Cf. F. Herman and S. Skillman, *Atomic Structure Calculations* (Prentice-Hall, Inc., Englewood Cliffs, New Jersey, 1963), pp. 1–8.

We also want to call attention to a related paper by Lindgren.[9] He uses an exchange potential with three parameters which are adjusted to minimize the expected value of the total energy.

The statistical approximation may be used for calculating the effects of correlation as well as exchange.[2] Calculations including correlation have been made by Tong and Sham.[10]

Note added in proof. It has been pointed out by Slater[11] that Gaspar[12] suggested the use of the smaller exchange potential and has done a number of calculations with it. Unfortunately he used a charge density based on the one obtained by the Thomas-Fermi method. The inaccuracies introduced thereby are similar in magnitude to the differences between the various self-consistent calculations reported here.

[9] I. Lindgren, Arkiv. Fys. (to be published). We are indebted to Dr. Lindgren for a copy of his report prior to publication.
[10] B. Y. Tong and L. J. Sham, preceding paper Phys. Rev. **144**, 1 (1966).
[11] J. C. Slater, Massachusetts Institute of Technology, Solid-State and Molecular Theory Group, Quarterly Progress Report, No. 58, 1965 (unpublished).
[12] R. Gaspar, Acta Phys. Hung. **3**, 263 (1954), and subsequent publications.

PHYSICAL REVIEW VOLUME 144, NUMBER 1 8 APRIL 1966

Lifetime, Coherence Narrowing, and Hyperfine Structure of the $(6s^26p7s)^3P_1^\circ$ State in Lead*

E. B. SALOMAN AND W. HAPPER
Columbia Radiation Laboratory, Columbia University, New York, New York
(Received 4 November 1965)

The lifetime and hyperfine structure of the $(6s^26p7s)\ ^3P_1^\circ$ excited state in lead have been investigated by the technique of level-crossing spectroscopy. The lifetime of the state was determined to be $\tau=5.75(20)\times10^{-9}$ sec. The linewidth of the level-crossing signal was observed to saturate at a "coherence-narrowed" value in agreement with theoretical predictions. The magnitude of this narrowing corresponds to a 27(3)% branching ratio to the ground state. When the branching ratio and the lifetime are combined with the $f(3639\text{ Å}):f(4058\text{ Å})$ oscillator-strength ratio measured by Khokhlov, one may infer the absolute f values: $f(2833\text{ Å})=0.169(17)$, $f(3639\text{ Å})=0.040(8)$, $f(4058\text{ Å})=0.155(31)$. The high-field level crossing in the hyperfine structure of the first $^3P_1^\circ$ state of Pb^{207} was found to occur at a magnetic field $H_c=4661.1(4)$ G, which corresponds to a magnetic-dipole-interaction constant $A=8.811(17)\times10^9$ cps.

I. INTRODUCTION

IN this paper we report on an experimental determination of the lifetime, coherence narrowing, and hyperfine structure of the $(6s^26p7s)^3P_1^\circ$ excited state in lead by level-crossing spectroscopy.

Precise values of the lifetime of an excited state of an atom and the related oscillator strengths (f values) are required by astrophysicists for studies of stellar structure and by plasma physicists for the determination of the properties of high-temperature plasmas. In addition, the experimental values provide a valuable check on approximation methods used to estimate atomic radiative properties. Knowledge of the oscillator strengths is needed in the calculation of emission and absorption probabilities, of resonant collision broadening of the optical line, of the collision broadening of level-crossing and double-resonance signals, and of the phenomenon of coherence narrowing. In the case of complex atoms, the observed lifetimes may be useful in determining the mixing of atomic states of different multiplicities.

* This work was supported wholly by the Joint Services Electronics Program (U. S. Army, U. S. Navy, and U. S. Air Force) under Contract No. DA-28-043 AMC-00099(E).

TABLE I. Theoretical and experimental values for the absorption oscillator strengths of lines originating in the $(6s^26p7s)^3P_1^\circ$ state of lead.

	Theoretical		Experimental					
λ (Å)	Bates and Damgaard[a]	Helliwell[b]	Corliss and Bozman[c]	Engler[d]	Khokhlov[e]	Bell and King[f]	Lifetime as reported here and Khokhlov's ratios	Lifetime as reported here and corrected f-value ratios reported here
2833	0.009	0.21	0.22(11)	0.6(1)	0.6(1)	0.23(2)	0.106(33)	0.169(17)
3639	0.014	0.089	0.09(5)		0.24(8)		0.042(14)	0.040(8)
4058	0.058	0.365	0.46(23)		0.92(36)		0.160(53)	0.155(31)

[a] Reference 6.
[b] Reference 7.
[c] Reference 3.
[d] Reference 1.
[e] Khokhlov only measured f-value ratios. He assumes Engler's f(2833-Å) value to obtain his absolute f values.
[f] Reference 2.

Several experiments have been performed to determine the oscillator strengths of the lines originating in the $(6s^26p7s)^3P_1^\circ$ state of lead. The atomic energy levels of interest are shown in Fig. 1. The values obtained by different workers are in serious disagreement. The f values determined by Engler[1] and by Bell and King[2] for the λ=2833-Å line in lead differ by a factor of 3. Both of these measurements were made by the atomic-beam-absorption method and therefore are subject to the uncertainties caused by the difficulty in determining the density of the absorbing particles in the atomic beam and in determining the spectral profile of the lamp. Corliss and Bozman[3] used a copper arc to measure the f values of all three lines originating in the $^3P_1^\circ$ state but do not claim more than 50% accuracy.[4] The relative f values were measured by Khokhlov[5] in a hollow-cathode lamp but are in some doubt because of self-absorption problems. This effect is expected to be most severe for the resonance line (2833 Å). The results of these measurements are summarized in Tables I and II.

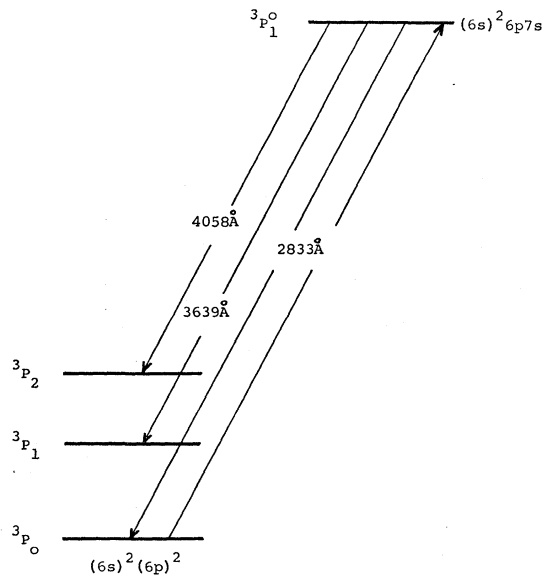

FIG. 1. Atomic energy levels of interest in lead.

Several methods have been used to calculate the f values, but their reliability is uncertain since accurate wave functions have not been computed for lead. The reliability of the Bates and Damgaard[6] Coulomb-approximation method is uncertain for an atom as heavy as lead. Helliwell[7] calculated the f values of all three lines using two-electron antisymmetrized wave functions, diagonalizing the matrix of the electrostatic and spin-orbit interactions, and evaluating the radial part of the wave function using WKB wave functions for a Thomas-Fermi potential. Helliwell's results are in substantial agreement with the absolute f value of Bell and King and the ratios of Khokhlov. The predictions of the theories of Bates and Damgaard and of Helliwell are listed in Tables I and III.

In view of the history of conflicting results and in spite of the apparent agreement between Helliwell and Bell and King, the present work was undertaken in the hope that it would provide definitive values for these radiative properties of lead. Similar recent studies have been made of the radiative lifetimes of the low-lying excited states of the alkali,[8–12] alkaline-earth,[13–16] and noble-gas atoms.[17] The present study is the first application of modern spectroscopic techniques to the carbon-group elements.

[1] H. D. Engler, Z. Physik **144**, 343 (1956).
[2] G. D. Bell and R. B. King, Astrophys. J. **133**, 718 (1961).
[3] C. H. Corliss and W. R. Bozman, Natl. Bur. Std. Monograph No. 53 (1962).
[4] W. R. Bozman (private communication).
[5] M. Z. Khokhlov, Contrib. Crimean Astrophys. Obs. **21**, 84 (1959); **22**, 118 (1960).
[6] D. R. Bates and A. Damgaard, Phil. Trans. Roy. Soc. (London) **A242**, 101 (1949).
[7] T. M. Helliwell, Astrophys. J. **133**, 566 (1961).
[8] H. Kruger and K. Scheffler, J. Phys. Radium **19**, 854 (1958).
[9] G. J. Ritter and G. W. Series, Proc. Roy. Soc. (London) **A238**, 473 (1957).
[10] U. Meyer-Berkhout, Z. Physik **141**, 185 (1955).
[11] K. Althoff, Z. Physik **141**, 33 (1955).
[12] K. C. Brog, thesis, Case Institute of Technology, 1963 (unpublished); H. Wieder, thesis, Case Institute of Technology, 1964 (unpublished).
[13] F. W. Byron, Jr., M. N. McDermott, and R. Novick, Phys. Rev. **134**, A615 (1964).
[14] F. W. Byron, Jr., M. N. McDermott, R. Novick, B. W. Perry, and E. B. Saloman, Phys. Rev. **134**, A47 (1964).
[15] A. Landman and R. Novick, Phys. Rev. **134**, A56 (1964).
[16] A. Lurio, R. L. deZafra, and R. J. Goshen, Phys. Rev. **134**, A1198 (1964).
[17] D. K. Anderson, Phys. Rev. **137**, A21 (1965).

Traditionally, excited states of atoms have been studied by the methods of optical spectroscopy. The resolution of the most precise spectroscopic instrument (the Fabry-Perot interferometer) can be made as small as 1 Mc/sec. Unfortunately, the useful resolution is generally limited by the Doppler broadening of the optical radiation. Typically, this limits the resolution to about 600 Mc/sec. Jackson[18] has partially overcome this difficulty through the use of an atomic beam, attaining linewidths as small as 30 Mc/sec. Unfortunately, the use of the atomic beam creates intensity problems which limit the applicability of the method. Radio-frequency techniques such as optical double resonance[19,20] reduce the linewidth problem by inducing transitions with radio-frequency photons whose Doppler width is much less than the natural linewidth. In this method the resonances are detected through their effect on the *intensity* of the optical radiation, and the optical Doppler broadening is circumvented. The sensitivity of the optical double-resonance technique is only limited by shot noise in the photon detector as opposed to conventional radio-frequency absorption methods, which are limited by thermal noise. Furthermore, since optical resonance scattering cross sections are many times greater than the geometrical cross section, one may excite the atom with high efficiency with resonance light. However, to cause radio-frequency transitions in short-lived states, one has the problem of providing sufficient radio-frequency power. For the $(6p7s)^3P_1°$ state in lead, an oscillating radio-frequency magnetic field amplitude of about 90 G is required to saturate the resonances. It is very difficult to obtain such a radio-frequency field without at the same time causing a discharge in the vapor. The level-crossing technique provides most of the advantages of the radio-frequency technique while completely eliminating the need for radio-frequency power. Since the level-crossing effect is an interference process which is detected through the change in the polarization or intensity of the lateral-scattered radiation, the output signal is not affected by Doppler broadening. The effect is analogous to double resonance at zero transition frequency. As with optical double resonance, optical (or ultraviolet) photons are detected and states are excited by resonance absorption with large cross sections. However, since a high-field level crossing occurs at one specific magnetic field, there is a search problem not present in double resonance. In the latter, the location of the resonance can be calculated for low magnetic fields from the known Landé g factor. The resonance can then be followed as the field is increased. In the case of the $^3P_1°$ state in lead, the level-crossing signal width is fairly broad because of the moderately short lifetime. This limits the precision of the determination but facilitates the location of the level-crossing field.

TABLE II. Lifetime of the $(6p7s)^3P_1°$ state as calculated from the measured oscillator strengths.

Oscillator strengths measured by	τ (sec)
Corliss and Bozman	$2.4(12)\times10^{-9}$
Engler with Khokhlov's ratios	$1.1(3)\times10^{-9}$
Bell and King with Khokhlov's ratios	$2.9(8)\times10^{-9}$

TABLE III. Prediction of lifetime of the $(6p7s)^3P_1°$ state of lead from theoretical oscillator strengths.

f values of	τ (sec)
Bates and Damgaard	21.0×10^{-9}
Helliwell	2.9×10^{-9}

The atomic energy levels of interest in lead are shown in Fig. 1. Lead atoms are excited from the $(6s^26p^2)^3P_0$ ground state to the $(6s^26p7s)^3P_1°$ state by $\lambda=2833$-Å resonance light. The $^3P_1°$ state then decays back either to the ground state or to the metastable $(6s^26p^2)^3P_1$ or $^3P_2$ states with the emission of $\lambda=3639$-Å or $\lambda=4058$-Å cross-fluorescent photons, respectively. The level crossing may be observed either in the fluorescent decay to the ground state or in either of the two cross-fluorescent decay modes. The branching to the $(6s^26p^2)^1D_2$ and $^1S_0$ states combined is calculated to be about 0.5% which is too small to affect the results of these experiments. We will not consider these branch modes any further.

The hyperfine structure and an independent determination of the lifetime of the $^3P_1°$ state were obtained from the high-field crossing of the hyperfine levels of Pb^{207}. The magnetic field dependence of the hyperfine

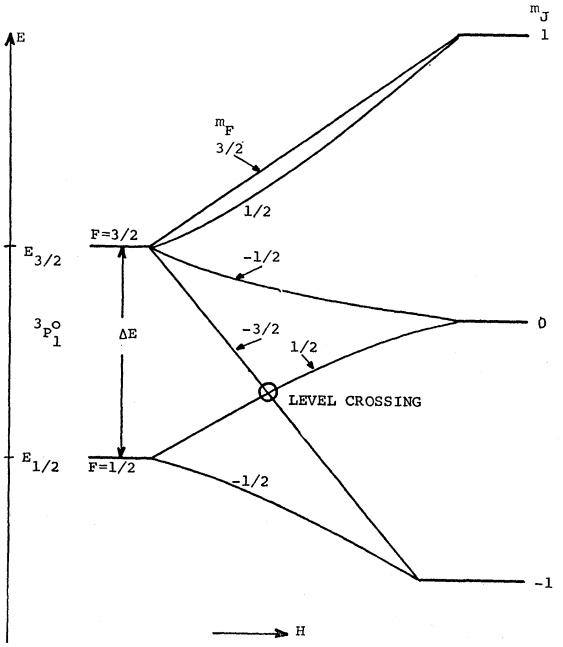

FIG. 2. Magnetic-field dependence of the hyperfine levels of the $^3P_1°$ state in Pb^{207}.

[18] D. A. Jackson, Proc. Roy. Soc. (London) **A263**, 289 (1961).
[19] J. Brossel and A. Kastler, Compt. Rend. **229**, 1213 (1949).
[20] J. Brossel and F. Bitter, Phys. Rev. **86**, 308 (1952).

levels of the $^3P_1°$ state in Pb^{207} are shown in Fig. 2. The magnetic field at which the crossing occurs served as a measure of the magnetic dipole interaction constant A in the excited state. The accuracy of this determination in the present experiments was limited by the uncertainty in g_J. Previous determinations of the hyperfine structure[21–23] using the methods of optical spectroscopy resulted in a value for the interaction constant A of $8.88(18)\times10^9$ cps.[24] The precision of this result is limited by the Doppler broadening of the observed line. The precision of a direct optical determination of A could only be improved through the use of an atomic beam absorber. In addition to the determination of A, the width of the high-field level crossing provided a valuable check on the lifetime of the excited state. Similar high-field level-crossing experiments with radioactive Pb^{205} could be used to investigate the hyperfine structure of that isotope and to obtain information about the nuclear moments.

In optical double-resonance or level-crossing experiments, one observes the intensity of scattered light as a function of some experimental parameter such as the static magnetic field. The width of the resulting signal can be used to measure the lifetime of the excited state. When the experimental conditions are such that an excited atom interacts only with the applied external fields during its decay, then the width determines the true radiative lifetime of the state. However, the linewidth can be affected by many extraneous factors, the most important of which are wall collisions, collisions with other atoms, and radiation trapping. Wall collisions were negligible in these experiments because of the very short distance that an excited lead atom can travel during its lifetime. However, effects due to radiation trapping and atom-atom collisions were observed. Radiation trapping generally causes a narrowing of the signal linewidth. This "coherence narrowing" can be understood from the following physical arguments. The Hanle effect may be described as the rotation of a classical damped oscillator (representing the radiating atom) in a magnetic field. If the magnetic field is strong enough to rotate the oscillator several times before its energy is dissipated, then the emitted light will be depolarized. Clearly a rapidly damping oscillator (an atom with a short lifetime) will require a larger magnetic field to depolarize the radiation pattern than a slowly damping oscillator so that the width of the Hanle-effect pattern is inversely proportional to the lifetime of the atom. When conditions are such that an atom can excite surrounding identical oscillators (multiple scattering), the orientation of the surrounding oscillators will reflect the orientation of the exciting oscillator. The surrounding oscillators will also precess in the magnetic field. As a result, a smaller magnetic field is required to depolarize the net radiation pattern, and the resulting Hanle-effect linewidth is narrowed.

In this work coherence narrowing in the presence of branching has been studied experimentally and theoretically. A review of previous work on the subject and a discussion of the peculiarities of the situation when branching is present are given in Sec. IIC.

II. THEORY

A. Level-Crossing Phenomena

The theory of the level-crossing phenomena has been formulated in different forms by Rose and Carovillano[25] and Franken.[26] It can be shown[27] that for a scattering direction perpendicular to both the incident light and the magnetic field, the $\Delta m_F=2$ level-crossing signal has a Lorentzian shape. In the experiments discussed below, phase-sensitive detection with Zeeman modulation was used. As a result, for small amplitude modulation, the observed signal was the derivative with respect to the magnetic field of the level-crossing signal. Thus, the shape of the observed signal resembles a dispersion curve. It is easy to show that the apparent lifetime of the atomic state is given by the following:

$$\tau=\frac{1}{\sqrt{3}\pi(\partial\nu/\partial H)\Delta H}, \tag{1}$$

where ΔH is the peak-to-peak separation of the dispersion shaped signal (in units of magnetic field), ν is the separation of the crossing levels (in units of frequency), and where the Zeeman slope $(\partial\nu/\partial H)$ is evaluated at the crossing field. In the case where the nuclear spin is zero and the two levels differ in m_F by two, Eq. (1) for the lifetime becomes

$$\tau=\frac{1}{\sqrt{3}\pi(2g_J\mu_0/h)\Delta H}, \tag{2}$$

where g_J is the Landé g factor of the atomic state, μ_0 is the Bohr magneton, and h is Planck's constant. For Pb^{207} the nuclear spin is $I=\frac{1}{2}$. In the $^3P_1°$ state, therefore, F is either $(\frac{3}{2})$ or $(\frac{1}{2})$. At zero field a $\Delta m=2$ level crossing is only possible within the $F=\frac{3}{2}$ levels. In this case, the lifetime is given by

$$\tau=\frac{1}{\sqrt{3}\pi\frac{2}{3}(2g_J\mu_0/h)\Delta H}. \tag{3}$$

The lifetime can also be determined from the observed width of the high-field level-crossing resonance in Pb^{207}. If one neglects the very small terms involving the

[21] H. Kopfermann, Z. Physik **75**, 363 (1932).
[22] J. L. Rose and L. P. Granath, Phys. Rev. **40**, 760 (1932).
[23] T. E. Manning, C. E. Anderson, and W. W. Watson, Phys. Rev. **78**, 417 (1950).
[24] P. Brix and H. Kopfermann, in *Landolt-Börnstein Tables*, edited by K. H. Hellwege (Springer-Verlag, Berlin, 1950), 6th ed., Vol. 1, Part 5, pp. 60–63.
[25] M. E. Rose and R. I. Carovillano, Phys. Rev. **122**, 1185 (1961).
[26] P. A. Franken, Phys. Rev. **121**, 508 (1961).
[27] A. Lurio and R. Novick, Phys. Rev. **134**, A608 (1964).

nuclear g factor g_I, a straightforward calculation again yields Eq. (3) as the expression for the lifetime.

B. Oscillator Strengths

Unfortunately, different authors have chosen to define the oscillator strength (f value) differently. In this paper the definition of the oscillator strength will be the same as that used by Condon and Shortley,[28] Mitchell and Zemansky,[29] and Foster.[30]

Consider the situation, as shown in Fig. 3 of a single upper state m and three lower states $n=1$, 2, 3 with statistical weights g_m and g_n, respectively. Photons of wavelength λ_n are emitted in the transition from m to n. Let the *absorption* oscillator strengths of the line λ_n be represented by f_n. Then, the coefficient for spontaneous emission from state m to state n is given by[29]

$$A_n{}^m=\frac{f_n}{1.499(g_m/g_n)\lambda_n{}^2},$$

where λ_n is measured in centimeters and $A_n{}^m$ is measured in inverse seconds. The lifetime of the excited state m, τ_m, is given by

$$\tau_m=1/(\sum_n A_n{}^m).$$

It can be shown that if the lifetime of the upper state has been directly determined and if the ratios of the f values are known to be

$$a=f_1/f_3, \quad b=f_2/f_3,$$

then the absolute value of the absorption oscillator strength for the λ_3 transition is given by

$$f_3=\left[\frac{1.499}{\tau_m}\right]\frac{g_m}{g_1 a/\lambda_1{}^2+g_2 b/\lambda_2{}^2+g_3/\lambda_3{}^2}, \tag{4}$$

where λ_n is measured in centimeters and τ_m is measured in seconds. The other two f values may be obtained from the known ratios a and b.

C. Coherence Narrowing with Branching

When multiple scattering of resonance photons becomes important, the widths of optical double-resonance and level-crossing signals are observed to narrow. This "coherence narrowing" is closely related to the phenomenon of radiation trapping[31,32] and reflects the increased lifetime of an ensemble of excited atoms in an optically thick vapor. Unrecognized coherence narrowing can cause errors in lifetime measurements by as much as a factor of three. On the other hand, the process is now well enough understood that one can use it to obtain information about the branching ratios from the resonance level of an atom like lead.

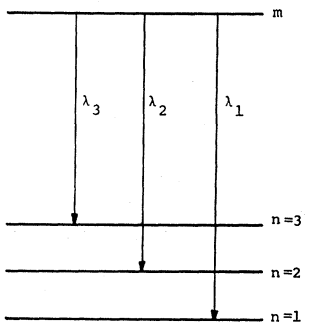

FIG. 3. Notation for the discussion of the relation of the absolute oscillator strengths to the lifetime.

The narrowing of optical double-resonance lines by multiple scattering was first described by Guiochon, Blamont and Brossel.[33] More detailed studies of the effect were carried out by Barrat,[34] who developed a theory of coherence narrowing using the density matrix formalism. Coherence narrowing in strong magnetic fields (optically separated Zeeman sublevels) was studied by Omont,[35] who showed that the theoretical maximum narrowing is greater for strong magnetic fields than for weak fields. This enhanced narrowing in strong fields was observed by Otten.[36] Another result of multiple scattering first considered by Omont[37] is a shift in the Larmor frequency of the resonance level. This is usually a negligible effect in practice. Dyakonov and Perel[38] effected a further refinement of the theory of coherence narrowing. By taking into account a more realistic velocity distribution than the monochromatic distribution used by Barrat, they obtained a relaxation time for randomly oriented excited atoms which is in good agreement with the results of Holstein. Their relaxation time for the "alignment"[39] (the quantity measured in Hanle-effect experiments when linearly polarized exciting light is used) is almost identical with that calculated by Barrat, the only difference being that the linewidth calculated by Dyakonov and Perel approaches its saturation value somewhat more slowly, with increasing vapor pressure, than in Barrat's theory. However, in both theories the saturation values of the linewidth are the same. Dyakonov and Perel also calculated the relaxation time for the "orientation"[39] (the "orientation" is a vector proportional to the magnetic moment of the excited atom). Omont[40] subsequently

[28] E. U. Condon and G. H. Shortley, *Theory of Atomic Spectra* (Cambridge University Press, Cambridge, 1953).
[29] A. Mitchell and M. Zemansky, *Resonance Radiation and Excited Atoms* (Cambridge University Press, Cambridge, 1961).
[30] E. W. Foster, Rept. Progr. Phys. **27**, 469 (1964).
[31] M. W. Zemansky, Phys. Rev. **29**, 513 (1927).
[32] T. Holstein, Phys. Rev. **72**, 1212 (1947).
[33] M. A. Guiochon, J. E. Blamont, and J. Brossel, Compt. Rend. **243**, 1859 (1956); J. Phys. Radium **18**, 99 (1957).
[34] J. P. Barrat, J. Phys. Radium **20**, 541 (1959); **20**, 633 (1959).
[35] A. Omont, Compt. Rend. **252**, 861 (1961).
[36] E. Otten, Naturwiss. **7**, 157 (1964).
[37] A. Omont, Compt. Rend. **258**, 1193 (1964).
[38] M. I. Dyakonov and V. I. Perel, Zh. Eksperim. i Teor. Fiz. **47**, 1483 (1964) [English transl.: Soviet Phys.—JETP **20**, 997 (1965)].
[39] W. Happer and E. B. Saloman, Phys. Rev. Letters **15**, 441 (1965).
[40] A. Omont, Compt. Rend. **260**, 3331 (1965).

measured the lifetimes of "alignment" and "orientation" in mercury vapor and found very good agreement with theory.

In the case of branching from the excited state, one can easily generalize Barrat's expression for the density matrix (see Appendix). The initial density matrix for optically excited atoms is composed of three terms $\rho^{(0)}$, $\rho^{(1)}$, and $\rho^{(2)}$ which describe the total "excitation," the "orientation," and the "alignment," respectively. The relaxation of the density matrix is then described by

$$\rho(t)=\sum_{L=0}^{2}\exp\left[-\Gamma\left(1-\sum_i x_i\alpha_i^{(L)}\frac{\Gamma_i}{\Gamma}\right)t\right]\times e^{-i\mathfrak{K}t}\rho^{(L)}(0)e^{i\mathfrak{K}t}. \quad (5)$$

Here Γ is the natural radiative lifetime of the state, Γ_i/Γ is the branching ratio for the ith branch, x_i is the trapping probability for photons associated with the ith branch, and $\alpha_i^{(L)}$ is an angular factor. The effective Hamiltonian in the rotating coordinate system is $\mathfrak{K}$. The precise expression for these quantities is given either in the Appendix or in the papers of Barrat.[34]

The intensity of detected photons of polarization λ in the ith branch is:

$$I_i(\lambda)\Delta\Omega=\Delta\Omega Z h\nu_i(1-x_i)\frac{3}{8\pi}\Gamma_i\sum_{\mu_i,m',m''}\langle\mu_i|\hat{e}_\lambda\cdot\mathbf{D}|m'\rangle\times\left[\int_0^\infty dt\, e^{-im'\omega t}\langle m'|\rho(t)|m''\rangle e^{im''\omega t}\right]\times\langle m''|\hat{e}_\lambda\cdot\mathbf{D}|\mu_i\rangle, \quad (6)$$

where $\Delta\Omega$ is the solid angle, Z is the number of atoms excited per second, ν_i is the frequency of the ith decay mode, μ_i represents the μth sublevel of the final state (branch state), m represents the sublevels of the excited state, $\mathbf{D}$ is the dipole operator, $\hat{e}_\lambda$ is the polarization vector, and $m\omega$ represents the Zeeman energy of the mth sublevel.

Several aspects of (5) and (6) are worth emphasizing here. The total intensity in the ith fluorescent mode is

$$I_i=\sum_\lambda\int_0^{4\pi}I_i(\lambda)d\Omega=\frac{h\nu_i Z(1-x_i)\Gamma_i}{\Gamma(1-\sum x_i\Gamma_i/\Gamma)}. \quad (7)$$

For a single decay mode (7) reduces to $I=h\nu Z$ which is obvious physically since all trapped photons must eventually escape. When several decay modes exist, the intensity in a strongly trapped branch approaches zero as the absorption probability x_i approaches unity. Most of the radiant energy escapes from the vapor in weakly trapped decay modes. In these experiments the resonance line in lead at 2833 Å was strongly trapped so that far better signals were obtained with the cross-fluorescent lines at 3639 and 4058 Å for which trapping was negligible.

Another less obvious aspect of branching concerns the relative signal intensity from $\rho^{(0)}$ and $\rho^{(2)}$. As we mentioned above, when there is no branching, the total intensity of scattered light is independent of the density of the vapor. However, from (5) and (6) we find that the ratio of the usable signal $I^{(2)}$ originating from $\rho^{(2)}$ to the isotropic unpolarized background signal $I^{(0)}$ which originates from $\rho^{(0)}$ is

$$\frac{I^{(2)}}{I^{(0)}}\approx\frac{\Gamma-\sum x_i\Gamma_i}{\Gamma-\sum x_i\Gamma_i\alpha_i}.$$

Since $\alpha_i<1$, the fraction of usable signal approaches zero when no branching is present. However, in the presence of branching, a significant fraction of polarized signal remains if at least one branch is not strongly trapped. These circumstances have made lead ideally suited for the investigation of coherence narrowing at high vapor densities.

From (5) and (6) we find that all decay modes exhibit the same coherence time:

$$T=\frac{\tau}{1-\sum x_i\alpha_i\Gamma_i/\Gamma}, \quad (8)$$

where τ is the true radiative lifetime of the excited state. Although one might naively expect that a strongly trapped decay mode would exhibit more coherence narrowing than a mode with little trapping, more careful consideration will show that this cannot occur since an atom which has trapped a resonance photon can reemit a cross-fluorescent photon. Our experiments confirm that all decay modes exhibit the same degree of narrowing at the same vapor pressure.

The degree of coherence narrowing at saturation may be used to obtain the branching ratio to the ground state. For the light intensities used in these experiments, no significant buildup of metastable atoms occurred so that the trapping probabilities x_1 and x_2 for the cross-fluorescent photons are zero. Thus, at saturation, Eq. (8) reduces to

$$\frac{\Gamma_0}{\Gamma}=\frac{10}{7}\left[1-\frac{\tau}{T_{2\infty}}\right]. \quad (9)$$

Here $T_{2\infty}$ is the apparent lifetime at saturation and Γ_0/Γ is the branching ratio to the ground state. This expression is independent of the vapor density and is also independent of the semiempirical characteristic length L of the cell.

An estimate of the reliability of Eq. (9) as a measurement of the branching ratio may be obtained by examining previous experimental work. Omont[40] observed a saturation value for the coherence narrowing in mercury which was 7% less than the theoretical maximum. Since the signal becomes very weak for a strongly trapped resonance line, this discrepancy may be due to experimental difficulties. If this is the case, one would

expect better agreement for lead since the cross-fluorescent signal remains quite strong even when the resonance line is almost completely trapped. However, the observed discrepancy may be due to an actual insufficiency in the theory since several of the approximations used to carry out the calculations are less reliable at higher atomic densities. We feel that the branching ratio obtained from Eq. (9) represents a lower limit to the real value. Moreover, judging from Omont's work, any possible systematic error arising from Eq. (9) is unlikely to cause more than a 10% underestimate of the branching ratio to the ground state.

III. EXPERIMENTAL APPARATUS

To observe the level-crossing effect, one requires only a source of resonance radiation, a magnetic field, a supply of scattering atoms, and a means of detecting the scattered light. In the following, the requirements of each of these components and the means by which they were met will be discussed.

A. Light Sources

The requirements for a good level-crossing light source are that the lamp provide a stable, intense, unself-reversed beam of light in the resonance line. In order to find a suitable light source for this work, three different types of lamp were considered. Because of the high temperatures required to obtain reasonable lead vapor pressures, it was initially thought that the hollow-cathode lamp[41,42] would be most suitable. However, it was found that light emitted from this lamp was not scattered by lead vapor. The reason for this is probably the self-absorption of the resonance line from the hollow-cathode lamp. Both Engler[1] and Khokhlov[5] observed this self-absorption when the lamp was operated at currents above 10 mA. In order to obtain sufficient intensity, currents of 200–600 mA are required. Variation of the lamp's operating conditions could not produce an intense unself-reversed output. No further discussion of the hollow-cathode lamp will be made here.

The next light source tried was of the electrodeless type. A few milligrams of high-purity lead were distilled into a quartz bulb of 3.2-cm diam, which had been cleaned in the manner described by McDermott and Novick.[43] About 10 Torr of argon was added to the bulb to initiate and maintain the discharge; the bulb was subsequently sealed off. The bulb was placed in the tank coil of a strongly driven Hartley oscillator so that about 100 W of power was coupled into the bulb. Asbestos and quartz wool were placed around the bulb as thermal insulation, allowing the bulb's temperature to rise to about 1000°C. At this temperature there was sufficient lead vapor pressure in the bulb for a reasonable intensity of $\lambda = 2833$-Å light to be emitted. The emitted light was considerably self-reversed due to the rather high oscillator strength of this line and the vapor pressure required for reasonable intensity. Measurements indicate that this lamp produces the equivalent of about 10^{11} unreversed photons/cm^2 sec at the absorption cell or an over-all effective power output of 200 μW in the $\lambda = 2833$-Å resonance line. In spite of this small power output, Hanle-effect resonances were observed with this lamp, and some of the experimental data discussed below were obtained with it. However, the signal-to-noise ratio is adversely affected by the low intensity. An increase in the lamp intensity by a factor of N increases the signal-to-noise ratio by a factor of $\sqrt{N}$.

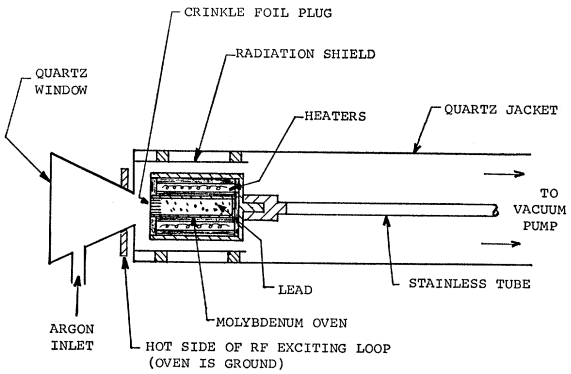

FIG. 4. Flow-lamp light source.

The most successful light source was of the flow lamp type.[41] As is shown in Fig. 4, it consists of a quartz tube through which an inert gas is pumped, an atomic beam oven which provides the lead atoms, and an rf discharge which excites the lead vapor. The quartz jacket consists of two sections, a rear cylindrical section which holds the oven and leads to the vacuum pump, and a front conical section with an inlet on its side for the inert gas. The conical section has an optical-grade quartz window on its front face to pass the ultraviolet light. The inert gas is argon, which is pumped directly from a large argon tank through an adjustable leak valve into the jacket and out again rather rapidly with a mechanical vacuum pump. A high flow rate is necessary to stop the heavy lead atoms before they deposit on the front window of the lamp. The pressure within the lamp was held constant during operation. Good performance was obtained at pressures between 1.6 and 4 Torr. The high temperatures required for the vaporization of lead required that considerable attention be given to the details of the design of the oven. A molybdenum beam oven with a molybdenum crinkle-foil plug was heated by a stainless-steel oven heater of the type designed by Lurio.[41] The heating elements of the oven heater were coiled 0.01-in.-diam tungsten wire through which current was driven by a H-Lab model 810B regulated power supply. Typical heating powers

[41] B. Budick, R. Novick, and A. Lurio, Appl. Opt. 4, 229 (1965).
[42] S. Tolansky, *High Resolution Spectroscopy* (Methuen and Company, Ltd., London, 1947).
[43] M. N. McDermott and R. Novick, Phys. Rev. **131**, 707 (1963).

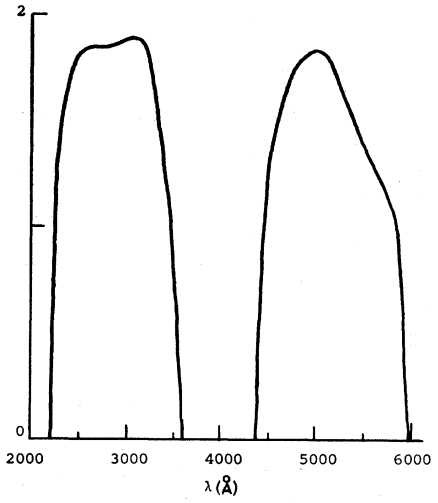

FIG. 5. Optical density as a function of wavelength for a 1 mole/liter $NiSO_4$ liquid absorption cell.

were in the range of 100–300 W. The oven heater was in turn surrounded by a tantalum radiation shield. With this arrangement, the oven could be heated to temperatures in excess of 900°C. The temperatures attained were sufficient to maximize the lamp output. The oven was loaded with 99.9999% pure lead shot. A 30 Mc rf discharge was maintained in the lamp by a Hewlett-Packard model 608D signal generator, an IFI model 500 wide-band amplifier, and a Boonton model 230-A tuned power amplifier together with a Johnson matching box. It was found necessary to use this elaborate system in order to maintain a stable discharge. The Hartley oscillator lamp exciter previously used[41] proved at times to be very sensitive to load changes in the lamp and would frequently change frequency causing the mode of the discharge in the lamp to change, thereby producing a fluctuation in the output of the lamp. This new rf system allowed stable long- and short-term operation of the lamp. Measurements with an Eppley thermopile indicate that this lamp produced about 3×10^{13} photons/cm²sec at the absorption cell corresponding to a total output power of about 10 mW.

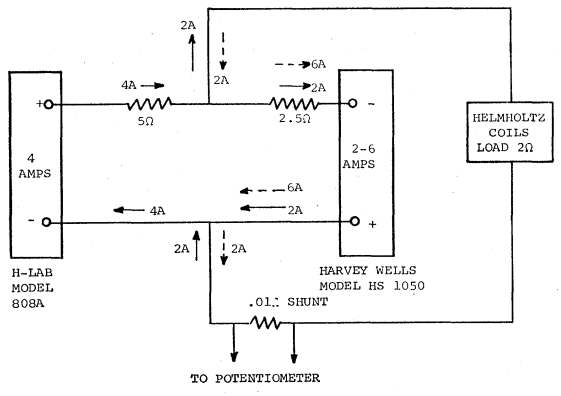

FIG. 6. Schematic of circuit used to power Helmholtz coils.

Using this lamp one can obtain a quite excellent signal-to-noise ratio in the Hanle-effect and high-field level-crossing signals. In addition, as will be discussed below, the flow lamp can readily be magnetically scanned.

The $\lambda=2833$-Å resonance line was isolated by a one-inch thick liquid absorption cell containing a solution of $NiSO_4$ with a concentration of 1 mole/liter. This absorption cell, whose optical density as a function of wavelength is shown in Fig. 5, transmits 75% of the $\lambda=2833$-Å light incident upon it while transmitting less than 1% of the $\lambda=3639$-Å and $\lambda=4058$-Å cross-fluorescent lines and the 2000–2100-Å resonance lines.

B. Zero-Field Level-Crossing Apparatus

1. Magnetic Field

A magnetic field varying between plus and minus 20 G is required to observe the zero-field level crossing (Hanle effect) in the $(6p7s)^3P_1^\circ$ state of lead. This field is produced by a 16-in. mean diameter Helmholtz coil pair whose field is homogeneous to one part in 30 000 over a region 1 in. in diameter. This homogeneity is far more than necessary for the short-lived states discussed herein. The magnetic field produced by these coils was calibrated as a function of the current passing through them by observing optical double resonances in the $^3P_1^\circ$ state of the even (nuclear spin zero) zinc isotopes. The slope of the calibration curve was determined to be 10.1220(5) G/A. In order to sweep through zero current, two current-regulated supplies were used as shown in Fig. 6. One of the supplies (*H*-Lab model 808A) supplied to a constant current of 4 A, while the other (Harvey-Wells model HS 1050) was swept from 2 to 6 A. This results in the current through the Helmholtz coils varying between +2 and −2 A without reversing the potential seen by either power supply. The current is determined by measuring the voltage drop across a precision 0.01Ω shunt on a Leeds and Northrup model K3 potentiometer. The magnetic field was modulated by means of modulation coils placed around the cell heating oven. A motor-driven potentiometer was used to sweep the Harvey-Wells power supply linearly over the range necessary to observe a level-crossing resonance.

In view of the finite integration time of the detector, the resonance line shape may be distorted by the Zeeman sweep. Byron[13] has shown that the apparent linewidth $\tilde{\Delta}_{1/2}$ is given by

$$\tilde{\Delta}_{1/2}\approx\Delta_{1/2}(1+6\beta^2),$$

where

$$\beta=\frac{\Delta_t}{\Delta_{1/2}}\frac{\tau_{RC}}{\tau_{sw}},$$

and Δ_t is the total range of the sweep, $\Delta_{1/2}$ is the full width at half-maximum of the incident Lorentzian-shaped signal, τ_{RC} is the effective time constant of the detection circuit, and τ_{sw} is the total time in which Δ_t is

swept out. In these experiments the detected line shape was a dispersion curve and $\Delta_{1/2}$ corresponds roughly to the peak-to-peak separation ΔH. The ratio τ_{RC}/τ_{sw} was held at about 1/180, while at worst $\Delta_t/\Delta H=3.5$. This corresponds to $\beta=0.01$ and a sweep correction of one part in 400, which is far less than the other uncertainties in these experiments. Thus we may neglect the finite sweep-rate correction.

2. Resonance Cell

The resonance cells were quartz cylinders 1 in. in diameter and 1 in. long on whose ends were sealed optical-grade quartz windows. The cells were baked under vacuum at a temperature of 1000°C, and then a few milligrams of lead, either 99.9999% chemically pure natural lead or 99.75% isotopically pure separated isotope Pb^{208}, were distilled into them. Further cleaning was achieved by sparking the cells with a Tesla coil before sealing them off at a pressure of about 10^{-6} Torr. The requirements for cell cleanliness are not as severe as for cadmium[13] and zinc[14] because of the short lifetime of the $^3P_1°$ state in lead.

The cells were heated electrically. Initially an oven made of type-304 "nonmagnetic" stainless steel was used to heat the cell, but for most of the work reported here an oven made of pure silver was used. Silver was used because its high heat conductivity would produce a uniform temperature over the total cell volume. In order to improve further the uniformity of the temperature over the cell, $\frac{7}{8}$-in.-diam slatted windows, as shown in Fig. 7, were used to allow light to enter and leave the cell oven. The slats allow most of the light normally incident on the window to enter the cell while considerably reducing the heat loss due to radiation. This is because the cell "sees" only hot silver around it except in small solid angles. The actual heating is provided by coiled 0.0126-in.-diam Nichrome wire which is powered from the 60-cycle power line with total power dissipations of about 600 W, which allows temperatures as high as 830°C to be reached. Temperature measurements were made with a platinum-platinum plus 10% rhodium thermocouple whose reference junction was maintained at 0°C in an ice-water bath. The thermocouple emf was measured with the Leeds and Northrup type-K3 potentiometer.

3. Detection System and Sensitivity

The detection system consists of high-quality quartz optics, a narrow-band interference filter with passband centered at either $\lambda=2833$ Å, $\lambda=3639$ Å, or $\lambda=4058$ Å, a light pipe, a Dumont K1306 photomultiplier (S-13 spectral response), a lock-in amplifier (narrow-band amplifier with phase-sensitive detection), and a Varian G-14 strip chart recorder. The quartz optics collects the light scattered at right angles to both the direction of the incident light and the direction of the magnetic field and passes it through one of the interference filters,

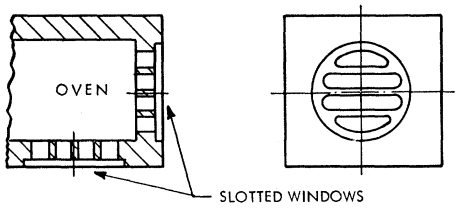

FIG. 7. Slatted cell-oven windows.

after which the monochromatic light is focused into the the light pipe which brings it to the photomultiplier. The component of the photomultiplier's output at the modulation frequency is amplified by the lock-in amplifier and displayed on the chart recorder. A schematic diagram of the zero-field level-crossing apparatus is shown in Fig. 8.

The sensitivity of this apparatus is such that a measurable line shape could be obtained with a three-second detection time constant for a density of 10^9 atoms/cm^3 in the 50 cm^3 cell. The sensitivity is limited primarily by lamp noise and by statistical fluctuations in the number of photons detected.

C. High-Field Level-Crossing Apparatus

1. Light Source

The flow-lamp light source described in Sec. IIIA provides sufficient light intensity to observe the high-field level-crossing effect. However, when it was used, no level crossing was observed. The reason for this can be seen in Fig. 9. which shows the theoretical lamp profile. The level crossing takes place one-third of the way from the Pb^{207} $F=\frac{1}{2}$ level to the Pb^{207} $F=\frac{3}{2}$ level. This position in the lamp profile is illuminated by no component of natural lead (at zero magnetic field), and hence no absorption of light by the crossing levels occurs. This difficulty can be overcome by magnetically displacing the lamp profile; this is accomplished by placing the emitting region of the lead flow lamp in a

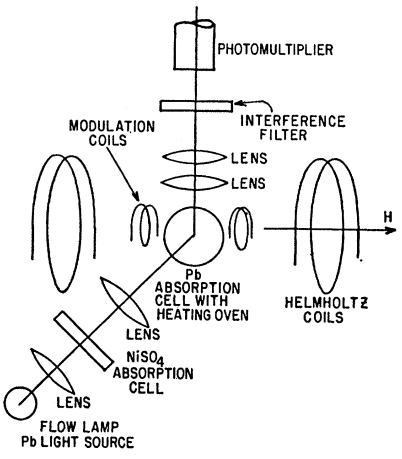

FIG. 8. Schematic diagram of zero-field level-crossing apparatus.

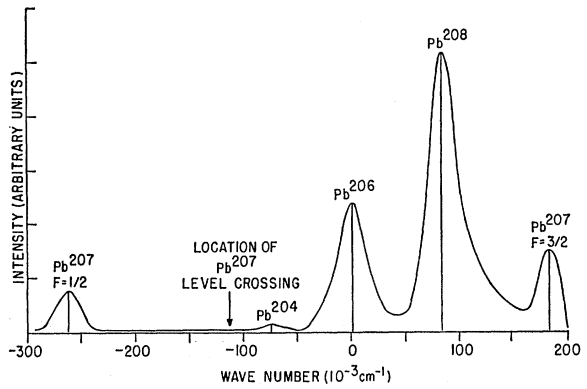

FIG. 9. Theoretical lead lamp profile.

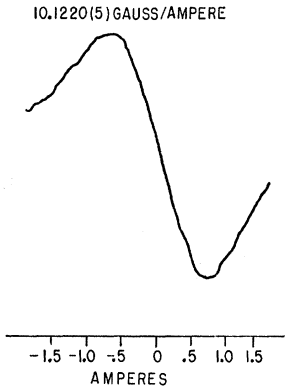

FIG. 11. Typical Hanle-effect resonance.

magnetic field of 3000 G. At this field, one of the three Zeeman components (σ light) of Pb^{208} lies very close to the location of the Pb^{207} level crossing. Since only σ light is involved in the $\Delta m=2$ high-field level-crossing effect, this 3000-G scanning field will enable one to observe the high-field level crossing. The 3000-G magnetic field was produced by a permanent magnet, with $2\frac{1}{4}$-in.-diam pole pieces and a $1\frac{3}{4}$-in. gap, which was magnetized to the desired field. The scanning magnetic field was parallel to the level-crossing field.

2. *Magnetic Field*

The high-field level crossing in the $(6p7s)^3P_1°$ state of Pb^{207} requires magnetic fields of the order of 5000 G. These fields were obtained by using a $6\frac{3}{4}$-in. iron-core electromagnet with a $2\frac{5}{16}$-in. gap. Current to the magnet's coils was provided by the Harvey-Wells model HS1050 power supply. Measurements indicated that the magnetic field was homogeneous to 1 G in 5000 G over a 1-in.-diameter region at the center of the magnet gap. This homogeneity is adequate for this experiment since the full width at half-maximum of the high-field level-crossing resonance is 22 G.

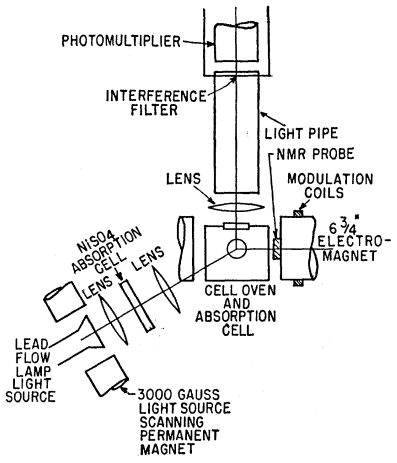

FIG. 10. Schematic diagram of high-field level-crossing apparatus.

The magnetic field is modulated at 37 cps by a coil on one of the magnet's pole pieces. One must be careful to keep the amplitude of this modulation low because the magnet will act as a transformer and couple the modulation back into the power supply. Such coupling impairs the performance of the current regulator.

The magnetic field is measured with a nuclear magnetic resonance (NMR) probe using glycerine as the sample. The probe is placed flat against one pole piece, and a calibration is made to relate the field at the pole piece to the field at the center of the gap where the absorption cell is situated. The calibration in the neighborhood of the level-crossing field is

$$H(\text{center})=0.999418(10)\times H(\text{pole piece}).$$

This result was obtained by taking the mean of ten determinations. The uncertainty in the calibration is one-tenth the uncertainty in the determination of the level-crossing field and so does not noticeably affect the precision of the field determination.

3. *Resonance Cell and Detection System*

The resonance cell and detection system used in measurements of the high-field level crossing were similar to those used for Hanle-effect measurements. A type-304 "nonmagnetic" stainless-steel oven heater was used to heat a natural lead cell. The detection system used another light pipe and a Dumont type-7664 photomultiplier (S-13 spectral response). A schematic diagram of the high-field level-crossing apparatus is shown in Fig. 10.

4. *Sensitivity*

The minimum temperature at which the level-crossing effect could be observed was 385°C. With allowance for the fact that the temperature was not measured at the coolest part of the cell, this corresponds to a Pb^{207} atomic density of about 2×10^8 atoms/cm^3 or 10^{10} Pb^{207} atoms in the vapor. This sensitivity is sufficient for work with radioactive isotopes. The sensitivity appears to be limited by statistical fluctuations in the number of photoelectrons collected in the photomultiplier.

IV. OBSERVATIONS

A. Lifetime of the $(6s^2 6p7s)^3P_1°$ State in Lead

The lifetime of the $(6s^2 6p7s)^3P_1°$ state in lead has been determined[44,45] in three separate measurements. In the first, the zero-field level-crossing apparatus described in Sec. III-B was used with a natural lead cell and the stainless-steel cell heating oven. Lead atoms were excited to the $(6p7s)^3P_1°$ state by $\lambda = 2833$-Å lead resonance light, and the 4058-Å fluorescent line from this state was detected. The resonance light was produced by the electrodeless lamp. Use of natural lead with its several isotopes results in a smaller coherence-narrowing effect than if a single isotope had been used. While all isotopes contribute to the Hanle-effect signal, coherence narrowing can occur only between atoms of the same isotope. This results from the large isotope shifts encountered in lead (see Fig. 9). A typical sample of data is shown in Fig. 11. As discussed above, the Hanle-effect resonance was observed with Zeeman modulation and phase-sensitive detection, and the observed signal is the derivative of the true resonance. Finite amplitude Zeeman modulation increases the apparent width of the level-crossing resonance. Lurio[46] has shown that the true width (ΔH) is related to the observed width ($\Delta H_{\rm obs}$) by

$$\Delta H = \frac{\Delta H_{\rm obs}}{1+0.75(\Delta\omega/\Gamma)^2},$$

where $\Delta\omega$ is the peak-to-peak modulation amplitude, and Γ is the full width at half-maximum of the Lorentzian level-crossing resonance. One plots either $\Delta H_{\rm obs}$ or $\Delta I_{\rm obs}$, the peak-to-peak separation in current units, versus the square of the modulation current (which is proportional to the square of $\Delta\omega$). The result

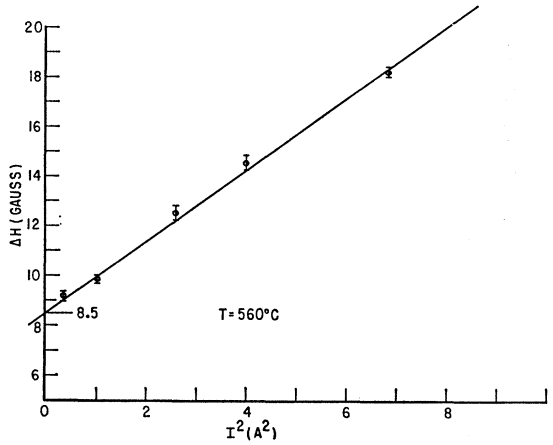

FIG. 12. Hanle-effect data: peak-to-peak separation as a function of modulation current.

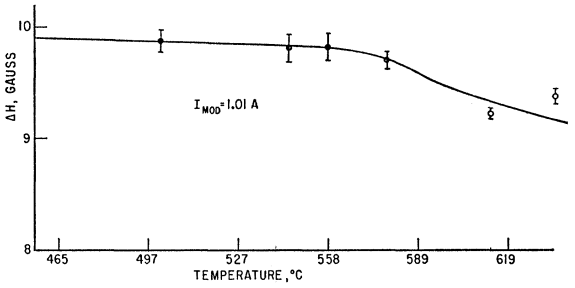

FIG. 13. Hanle-effect data: peak-to-peak separation as a function of temperature.

is a straight line whose intercept at zero current is the corrected peak-to-peak separation ΔH. This is shown in Fig. 12. The effect of coherence narrowing can be determined by plotting the peak-to-peak separation as a function of cell temperature at fixed modulation amplitude. The result, shown in Fig. 13, exhibits a small coherence-narrowing effect. While the procedure of using constant modulation amplitude is not precisely correct, it was adequate for the evaluation of the small corrections needed to account for the coherence narrowing in the lifetime determination with natural lead. When separated isotopes were used, a larger coherence-narrowing effect was observed and a more elaborate procedure was employed. The coherence-narrowing data obtained with natural lead could not be used for a precise study of the coherence-narrowing effect since the stainless-steel cell oven did not heat the cell uniformly, and therefore the density of the atoms in the cell was only poorly known. The lifetime of the state is calculated from the peak-to-peak separation by using Eq. (2). It was necessary to correct this lifetime value for the coherence-narrowing effect and for the presence of Pb^{207} (nuclear spin $I=\frac{1}{2}$) in the natural-lead absorption cell. Equation (3) shows that the Pb^{207} Hanle-effect signal is 1.5 times broader than the even isotope Hanle-effect signal. An analysis of the effect of the presence of the odd isotope was made by adding the signal expected from Pb^{207} to that expected from the even isotopes. The intensities of the isotopes were added in the ratio of their abundances in the absorption cell. It was found that the width of the combined curve was 4% greater than that for the even isotopes alone. Therefore, a 4% correction was indicated. This correction was calculated

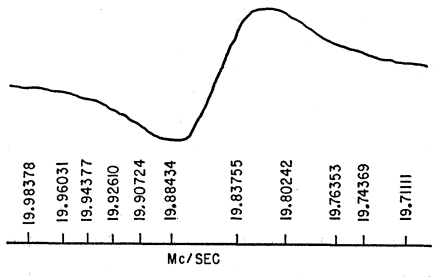

FIG. 14. Typical high-field level-crossing resonance.

[44] R. Novick, B. W. Perry, and E. B. Saloman, Bull. Am. Phys. Soc. 9, 625 (1964).
[45] E. B. Saloman, Bull. Am. Phys. Soc. 10, 49 (1965).
[46] A. Lurio (private communication).

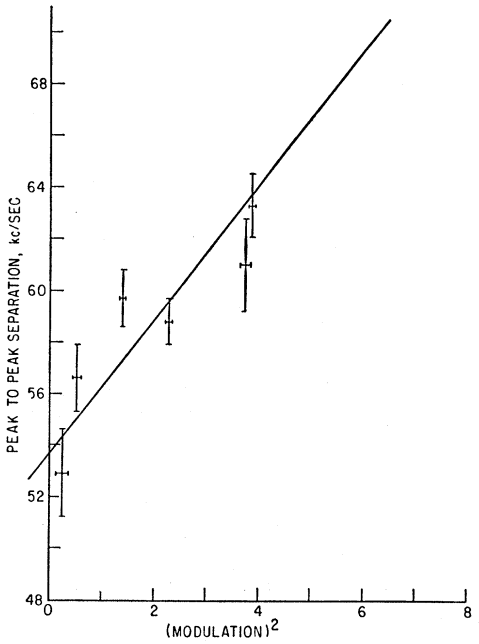

FIG. 15. High-field level-crossing data: peak-to-peak separation as a function of modulation amplitude.

under the assumption that the odd isotope's spectral components suffered the same degree of self-reversal as those of the even isotopes. The lifetime of the $(6p7s)^3P_1^\circ$ state as obtained by this procedure is

$$\tau = 5.8(4) \times 10^{-9} \text{ sec},$$

where the quoted uncertainty is twice the standard deviation of the data.

In the second set of measurements, the high-field level-crossing effect was used to determine the lifetime of the $(6p7s)^3P_1^\circ$ state in lead. The same natural lead cell and stainless-steel oven described above were used in high-field level-crossing apparatus described in Sec. IIIC. The $^3P_1^\circ$ state was excited by $\lambda = 2833$-Å resonance light from the magnetically displaced flow lamp, and the level crossing was detected in the $\lambda = 2833$-Å fluorescence. Since only one isotope of natural lead has a high-field level crossing, there can be no confusion from mixtures of the signals from the even isotopes with that from the odd isotope as was possible in the first determination. Due to the large isotope shifts of the various lead isotopes, coherence-narrowing effects can occur only between atoms of the same isotope. Since only 21% of natural lead is Pb^{207}, one would roughly expect that the coherence-narrowing effect would be only about 4% of that observed with pure Pb^{208}. Thus we would expect less than a 1% coherence-narrowing effect. This was confirmed experimentally by observing the width of the level-crossing signal at temperatures corresponding to a change in atomic density of about ten. No change was observed to within the statistical uncertainty of 2%. Typical high-field level-crossing data are shown in Fig. 14 in which the field markers are given in terms of the proton NMR frequency. The observed peak-to-peak separations were plotted against the square of the modulation amplitude as shown in Fig. 15. When extrapolated to zero modulation and corrected for the off-centered NMR probe, the width of the level-crossing signal is observed to be 12.6(4) G, which, through the use of Eq. (3), corresponds to a lifetime for the $(6p7s)^3P_1^\circ$ state of

$$\tau = 5.8(2) \times 10^{-9} \text{ sec}.$$

In the third measurement, the lifetime was redetermined with the Hanle effect, using a cell which contained 99.75% isotopically pure Pb^{208}, thus eliminating the correction for the presence of the odd isotope. The cell was uniformly heated in the silver-cell oven described above. The high isotopic purity made the coherence-narrowing effect particularly pronounced. This effect was compensated for by lowering the atomic density to 1.8×10^9 atoms/cm³ in the 50-cm³ cell and by extrapolating the linewidth to zero density. The $^3P_1^\circ$ state was excited by $\lambda = 2833$-Å light from the flow lamp, and the $\lambda = 3639$-Å cross-fluorescent decay was detected. A plot of peak-to-peak separation versus modulation is shown in Fig. 16 for the lowest density used. Figure 17 shows the peak-to-peak separation extrapolated to zero modulation as a function of atomic density within the absorption cell. At each temperature, observations were made with at least four different values of the modulation amplitude; at least six resonances were obtained for each value of the modulation. From Fig. 17 and the

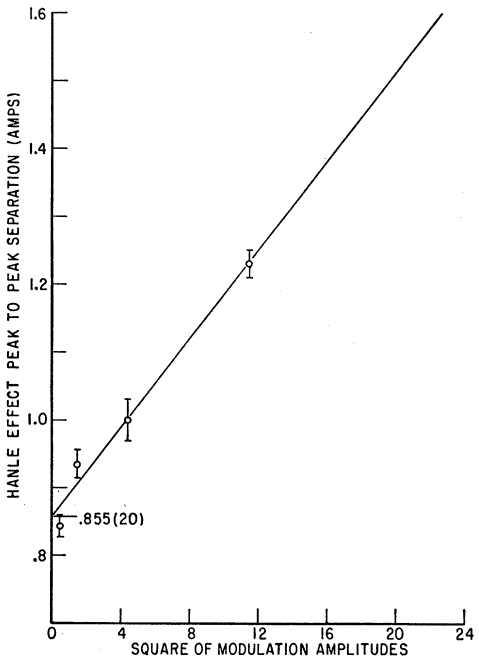

FIG. 16. Hanle-effect data: peak-to-peak separation as a function of modulation amplitude.

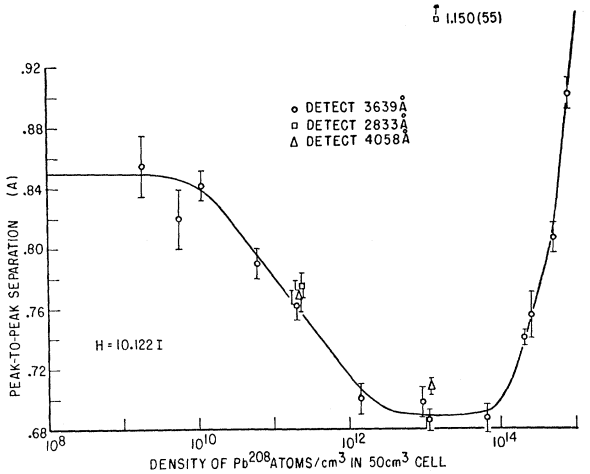

FIG. 17. Hanle-effect data: peak-to-peak separation as a function of density. Coherence-narrowing and collision-broadening effects.

known Helmholtz-coil calibration, we obtained for the peak-to-peak separation at low densities the value 8.6(3) G, which corresponds to a lifetime for the $(6p7s)^3P_1^\circ$ state of

$$\tau = 5.7(2) \times 10^{-9} \text{ sec}.$$

All determinations of the lifetime of the $^3P_1^\circ$ state agree to well within their estimated uncertainties.

B. Coherence Narrowing

The linewidth data[39,47] contained in Fig. 17 display, for the first time, the saturation of coherence narrowing predicted by Barrat.[34] In this figure the effect of coherence narrowing is indicated by the reduction of the linewidth as the atomic density is increased from 10^9 atoms/cm^3 to 10^{14} atoms/cm^3. The rapid increase in linewidth at densities above 10^{14} is attributed to collision broadening and will be discussed in a later paper. The linewidth observed under conditions of saturated coherence narrowing was 81% of the free-atom (zero-density) value. The intensity of the level-crossing signal as observed with the 3639 and 4058-Å cross-fluorescent lines was essentially constant and independent of density at densities greater than about 10^{11} atoms/cm^3. The intensity obtained with the 2833-Å resonance line decreased in this density region, and the line became essentially unobservable at densities greater than about 10^{14} atoms/cm^3. These observations are in agreement with the predictions made in Sec. IIC.

Equation (9) for the branching ratio is valid only if the $(6p^2)^3P_1$ and $(6p^2)^3P_2$ metastable states are unpopulated. Under the conditions of the present experiment, these states are populated through the decay of the $(6p7s)^3P_1^\circ$ state and are depopulated by wall collisions. In the limit of high density (large absorption of the incident 2833-Å resonance radiation), each 2833-Å photon produces a metastable atom. With the present light sources, at most, 6×10^{13} photons/sec are incident on the bulb, and the metastable population, therefore, never exceeds about 5×10^9 atoms. Such a population will not trap the cross-fluorescent radiation. To verify this estimate, the width of the level-crossing signal was studied as a function of the light intensity. No change in the linewidth was observed for incident light intensities differing by a factor of 10. As noted above, each point of Fig. 17 is the result of at least six level-crossing resonances at each of four or five modulation field amplitudes. It was shown in Sec. IIC that the degree of narrowing depends on the excited-state branching ratio. By using Eq. (9) one finds that the observed narrowing corresponds to a 27% branching ratio to the ground state $(6p^2)^3P_0$. This result is in disagreement with the value obtained from Khokhlov's f-value ratios.[5] Using the theory of Dyakonov and Perel[38] with a 27% branching ratio and with $L=2.1$ cm, we can predict the form of the coherence-narrowing curve. The results of such a prediction are shown in Fig. 18 together with the experimental points and are discussed in Sec. VC.

The widths of the Hanle-effect signals as detected with the various decay modes of the $^3P_1^\circ$ state were compared at two values of the atomic density, one on the slope of the coherence-narrowing curve and the other where the coherence-narrowing curve saturates. At the lower density (2×10^{11} atoms/cm^3), on the slope of the coherence-narrowing curve, the signals of all three decay modes had the same width to within their statistical uncertainties. The results at the higher density (10^{13} atoms/cm^3) for the cross-fluorescent lines $\lambda=3639$ Å and $\lambda=4058$ Å also agree; however, the peak-to-peak separation in the $\lambda=2833$-Å resonance line was greater by 60% than that obtained with the other lines. However, it is important to recognize that the absorption depth for the 2833-Å line is only about 0.01 cm at this density, while the cell diameter is about 2.5 cm. It is suggested that the 2833-Å signal arises from

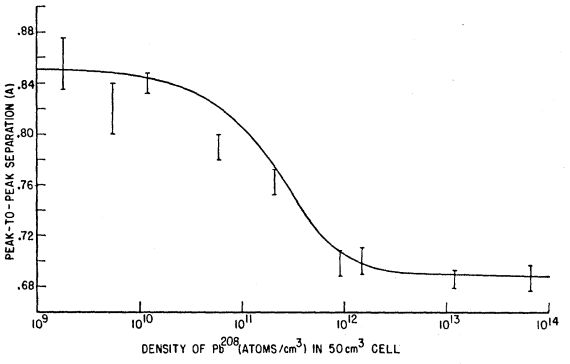

FIG. 18. Experimental points with the curve of the coherence-narrowing effect predicted by Dyakonov and Perel with branching ratio equal to 27% and $L=2.1$ cm.

[47] E. B. Saloman and W. Happer, Bull. Am. Phys. Soc. **10**, 596 (1965).

TABLE IV. Results: Lifetime of the $(6p7s)^3P_1^\circ$ state of Pb.

Method	Value (10^{-9} sec)
1. Hanle effect with natural isotope ratio and an estimated 4% correction for odd-spin isotope.	5.8(4)
2. Width of high-field level crossing in Pb^{207}.	5.8(2)
3. Hanle effect in separated 99.75% Pb^{208}.	5.7(2)

atoms close to the entrance window of the cell and that the fluorescent photons reach the detector through multiple internal reflections within the cell walls. Under these conditions we might expect the line shape to be modified. To confirm this the oven geometry was changed in order to increase the probability that 2833-Å photons reach the photomultiplier by a direct path through the cell. It was found that now the peak-to-peak separation was only 13% broader than that for the cross-fluorescent lines. This supports our interpretation of this effect. The cross-fluorescent photons can propagate through the body of the cell without absorption, and hence we expect no anomalous effects in these signals.

C. High-Field Level Crossing

Two determinations were made of the high-field level crossing in the $(6p7s)^3P_1^\circ$ state of Pb^{207}. In the first determination,[44] a total of 40 resonances was observed by detecting the $\lambda=4058$-Å cross-fluorescent decay. The signal-to-noise ratio was about 7 to 1 in this series of measurements. The results obtained for the level-crossing field were

$$H_c=4661(2)\text{ G},$$

where the quoted uncertainty is twice the statistical uncertainty. The location of the high-field level crossing was redetermined by detecting the $\lambda=2833$-Å decay mode after the apparatus had been carefully optimized. A typical resonance curve for this line is shown in Fig. 14. From the observation of a total of 43 resonances, the level-crossing field was determined to be

$$H_c=4661.1(4)\text{ G},$$

where the quoted uncertainty is twice the statistical uncertainty. In Sec. VD, we evaluate the hyperfine structure coupling constant from these results.

V. CONCLUSIONS

A. Lifetime of the $(6s^26p7s)^3P_1^\circ$ State in Lead

A summary of the results from the three determinations of the lifetime of the $(6s^26p7s)^3P_1^\circ$ state in lead is given in Table IV. All determinations agree to within their assigned uncertainties. The weighted mean of these determinations for the lifetime of the $^3P_1^\circ$ state is

$$\tau=5.75(20)\times10^{-9}\text{ sec}.$$

It is important to note that this lifetime value is independent of our knowledge of the density of lead atoms in the absorption cell and of the spectral profile of the resonance lamp. The determination of the density constitutes the prime source of uncertainty in the determination of the lifetime by atomic-absorption methods. In the absorption methods, the spectral profile of the resonance lamp introduces further uncertainties. All previous determinations of the lifetime of the $^3P_1^\circ$ state in lead were subject to these uncertainties.

B. Oscillator Strengths

As noted in Sec. IIB, if one knows the lifetime of an excited state and the ratios of the f values of all spectral lines originating in this state, one may then calculate the absolute f values from Eq. (4). Khokhlov[5] has measured the f-value ratios, and he reports

$$f(2833\text{ Å}):f(3639\text{ Å}):f(4058\text{ Å})=0.65(22):0.26(9):1.00,$$

which implies a branching ratio of 17(6)% to the ground state. This branching ratio is not consistent with the observed coherence narrowing. Even so, it is of interest to evaluate the f values with the ratios given by Khokhlov. In this way we obtain

$$f(2833\text{ Å})=0.106(33),$$
$$f(3639\text{ Å})=0.042(14),$$
$$f(4058\text{ Å})=0.160(53).$$

However, as reported in Sec. IVB, the saturation value of the coherence-narrowing effect implies a branching ratio to the ground state of 27%. It is reasonable to assume that the difference between the branching ratio found here and that found by Khokhlov arises from self-absorption effects in Khokhlov's experiments. These would primarily affect the ratios involving the $\lambda=2833$-Å resonance line. If one assumes that Khokhlov's $f(3639\text{ Å}):f(4058\text{ Å})$ ratio is correct, and if we use the present ground-state branching ratio, we find that the f-value ratios are

$$f(2833\text{ Å}):f(3639\text{ Å}):f(4058\text{ Å})=1.09:0.26:1.00$$

which, when combined with the lifetime, correspond to the absolute f values:

$$f(2833\text{ Å})=0.169,$$
$$f(3639\text{ Å})=0.040,$$
$$f(4058\text{ Å})=0.155.$$

$f(2833\text{ Å})$ is independent of Khokhlov's ratios and is good to 11%. We estimate that the other two values are reliable to about 20%.

Indications that Khokhlov's f-value ratios are incorrect were observed several times during the course of this work. The high-field level-crossing signals observed in the $\lambda=4058$-Å fluorescence were much weaker than

they were in the other two decay modes contrary to what would be expected if Khokhlov's ratios were correct. Similar discrepancies were observed in the zero-field level-crossing signals and in the predicted narrowing of the linewidth by the coherence-narrowing effect.

In Table I the oscillator strengths obtained above are compared with those obtained in other experimental determinations and those calculated by several theoretical methods. The last column of Table I gives the f values as determined from our measured lifetime and branching ratio to the ground state, using only Khokhlov's $f(3639\text{ Å}):f(4058\text{ Å})$ ratio. In the next-to-the-last column are the f values determined when the measured lifetime is combined with all three of Khokhlov's f-value ratios. The other columns list the theoretical and experimental f values determined by others. The Bates and Damgaard Coulomb-approximation value is not expected to be reliable for an atom as heavy as lead. Helliwell's calculated ratios[7] agree with Khokhlov's and hence do not agree with the branching to the ground state determined here. The f values obtained by Corliss and Bozman[3] agree with those we have obtained (last column) for two of the three lines; however, their values are estimated to be reliable only to a factor of 2 for nonresonance lines and a considerably larger factor for resonance lines.[4] Engler's $f(2833\text{ Å})$ value is in disagreement with all other measurements. Khokhlov measured only ratios and obtained his absolute f values by assuming Engler's $f(2833\text{ Å})$ value. Bell and King have determined the $f(2833\text{ Å})$ value, and their result agrees with the result we obtained (last column) to within the quoted uncertainties.

C. Coherence Narrowing

The observed coherence narrowing is in essential agreement with the theory as represented by Eq. (8) if one chooses the semiempirical parameter (L) to be 2.1 cm and the branching ratio to the ground state to be 27%. As can be seen from Fig. 18, the experimental points and the theoretical curve begin to decrease at the same density (due to the choice of L), saturate at the same peak-to-peak separation (due to the choice of branching ratio), and the narrowing takes place over the predicted range of densities. It appears that the theory is in reasonable agreement with the experimental results, although there is a slight disagreement in the shape of the curve in the density region of 10^{11} atoms/cm^3.

D. Magnetic Dipole Interaction Constant for the $(6s^2 6p\,7s)^3P_1^\circ$ State in Pb^{207}

The magnetic-dipole-interaction constant (A) for the $(6s^2 6p\,7s)^3P_1^\circ$ state in Pb^{207} is related to the crossing field (H_c) and the Landé g factor (g_J) by[48]

$$A=g_J\mu_0 H_c/h,$$

where μ_0 and h have their usual meanings. This formula neglects second-order corrections arising from the presence of the $(6p7s)^3P_0^\circ$ and $(6p7s)^3P_2^\circ$ states. These corrections are much smaller than uncertainties arising from our limited knowledge of the g factor. The best available value of g_J is that of Back,[49] who obtained

$$g_J=1.349(3)$$

by optical Zeeman spectroscopy. Taking

$$H_c=4661.1(4)\text{ G}$$

as given above, we find

$$A=8.811(17)\times 10^9\text{ cps}.$$

This result is in good agreement with the optical-spectroscopic value[24]

$$A=8.88(18)\times 10^9\text{ cps}.$$

The uncertainty in the present result arises almost entirely from that in g_J.

ACKNOWLEDGMENTS

The authors wish to thank Professor Robert Novick for his assistance and encouragement during the course of this work. They wish to thank Dr. B. W. Perry for his aid in the early stages of these experiments. They would also like to thank the staff of the Columbia Radiation Laboratory for their interest and unfailing assistance.

APPENDIX

Barrat's coherence-narrowing theory may be extended to the case where branching is present in the following manner. Consider an ensemble of N identical atoms. An excited atom can decay to any one of r lower lying levels. Then (II.1) of Ref. 34 becomes

$$\begin{aligned}&i\frac{d}{dt}A[1i_1\mu_1\cdots ne,\cdots Ni_N\mu_N;t]\\&=[k_0-i(\Gamma/2)+\mathfrak{IC}]A[1i_1\mu_1\cdots ne,\cdots Ni_N\mu_N;t]\\&\quad+i\sum C(n'i_{n'}\mu_{n'};ni_{n'}\mu_n t)e^{i\alpha_{n'n}t}\\&\quad\times A[1i_1\mu_1;\cdots ni_{n'}\mu_n\cdots n'e\cdots Ni_N\mu_N;t].\end{aligned}$$

The state vectors now require an additional label i_n to designate the terminal-state multiplet. All other notation is identical to that of Ref. 34. One must generalize the concept of a path of order p to take into account the various ways in which one state vector may be coupled to another by the exchange of p photons. For instance, if $p-1$ photons of the type k_i and one photon of the type k_j are exchanged, then the photon k_j may be inserted in the sequence of photons k_i in any one of p distinct positions so we assign a weight of p to this

[48] P. Thaddeus and R. Novick, Phys. Rev. **126**, 1774 (1962).

[49] E. Back, Z. Physik **37**, 193 (1926); **43**, 317 (1927).

TABLE V. Depolarization factors of multipolarity one. $\alpha^{(L)}$, $L=1$.

J \ J'	0	1	2	3	4
0	0	1/2	0	0	0
1	0	1/8	3/8	0	0
2	0	1/8	1/24	1/3	0
3	0	0	1/6	1/48	5/16
4	0	0	0	3/16	1/80

J \ J'	1/2	3/2	5/2	7/2
1/2	1/3	5/12	0	0
3/2	1/12	1/15	7/20	0
5/2	0	3/20	1/35	9/28
7/2	0	0	5/28	1/63

sort of path. In general, we denote a path corresponding to the exchange of n_1 photons k_1, $\cdots$, n_r photons k_r by $[n_i]$. Then the weight $W([n_i])$ of a path $[n_i]$ is just the coefficient of $\prod_{i=1}^{r}(k_i)^{n_i}$ in the expansion of $(k_1+k_2+\cdots k_r)^P$, i.e.,

$$\sum_{[n_i]} W([n_i])\prod_{i=1}^{r}(k_i)^{n_i}=(\sum_{i=1}^{r}k_i)^P.$$

After summing over "squared" terms and including the effects of the paths C', we find that in (II.17) of Ref. 34

TABLE VI. Depolarization factors of multipolarity two. $\alpha^{(L)}$, $L=2$.

J \ J'	0	1	2	3	4
0	0	7/10	0	0	0
1	0	7/40	147/600	0	0
2	0	7/1000	147/600	21/125	0
3	0	0	1/50	21/80	11/80
4	0	0	0	7/240	539/2000

J \ J'	1/2	3/2	5/2	7/2
1/2	0	7/20	0	0
3/2	0	28/125	49/250	0
5/2	0	7/500	32/125	3/20
7/2	0	0	1/40	4/15

we must make the replacement

$$\left[\frac{9x\Gamma}{8\pi(2F+1)}\right]^p\times\cdots\longrightarrow\sum_{[n_i]}W([n_i])\times\prod_{i=1}^{r}\left[\frac{9x_i\Gamma_i}{8\pi(2F+1)}\right]^{n_i}\times\cdots.$$

The remaining manipulations are straightforward and result in a density matrix of the form

$$\rho(t)=\sum_L\exp\left[-\Gamma\left(1-\sum_{i=1}^{r}x_i\alpha_i^{(L)}\frac{\Gamma_i}{\Gamma}\right)t\right]e^{-i\mathcal{H}t}\rho^{(L)}(0)e^{i\mathcal{H}t},$$

where

$$x_i=1-e^{-2K_iN_iL},$$

$$K_i=\frac{\pi^2}{4}\frac{2F+1}{2I_i+1}\times\frac{\Gamma_i}{k_i^3v}.$$

The branching ratio to the ith level is Γ_i/Γ. It is convenient to specify the initial density matrix $\rho(0)$ in terms of Fano's[50] irreducible tensors $T_M{}^L$ so that

$$\rho(0)=\sum_L\sum_M\mathrm{Tr}\{\rho(0)T_M{}^{L\dagger}\}T_M{}^L=\sum_L\rho^{(L)}(0).$$

A general expression for the depolarization factors $\alpha^{(L)}$ is

$$\alpha^{(L)}=-\frac{9}{2}\left\{\frac{1}{3}+\frac{C^2(11L;000)}{2L+1}\right\}(2J'+1)W^2(11J'J';LJ),$$

where the Clebsch-Gordan coefficients (Rose's notation) and Racah coefficients are tabulated. J' is the angular momentum of the excited state, and J is the angular momentum of the state to which the atom decays. Using the above equation and the orthogonality relations for the Racah coefficients, one can easily show that $\alpha^{(0)}=1$. $\alpha^{(1)}<1$, $\alpha^{(2)}<1$, and $\alpha^{(L)}=0$ for $L>2$. We have listed $\alpha^{(1)}$ and $\alpha^{(2)}$ for low values of J and J' in Tables V and VI. The theory of coherence narrowing with branching discussed above applies equally well to atoms with well-resolved hyperfine levels in the ground state such as thallium.

[50] U. Fano, Rev. Mod. Phys. **29**, 74 (1957).